Published in final edited form as:
Cortex. 2014 September ; 58: 139–150. doi:10.1016/j.cortex.2014.05.014.

White matter microstructure complements morphometry for predicting verbal memory in epilepsy

Carrie R. McDonald[a,b], **Kelly M. Leyden**[b], **Donald J. Hagler Jr**[b,c], **Nuri E. Kucukboyaci**[b,d], **Nobuko Kemmotsu**[a,b], **Evelyn S. Tecoma**[e], and **Vicente J. Iragui**[e]

[a]Department of Psychiatry, University of California, San Diego, 9500 Gilman Drive, La Jolla, CA, 92037, USA

[b]Multimodal Imaging Laboratory, University of California, San Diego, 8950 Villa La Jolla Drive, La Jolla, CA, 92037, USA

[c]Department of Radiology, University of California, San Diego, 9500 Gilman Drive, La Jolla, CA, 92037, USA

[d]San Diego State University/University of California, San Diego Joint Doctoral Program in Clinical Psychology, San Diego, CA, USA

[e]Department of Neurosciences, University of California, San Diego, La Jolla, CA, USA

Abstract

Verbal memory is the most commonly impaired cognitive domain in patients with temporal lobe epilepsy (TLE). Although damage to the hippocampus and adjacent temporal lobe structures is known to contribute to memory impairment, little is known of the relative contributions of white versus gray matter structures, or whether *microstructural* versus *morphometric* measures of temporal lobe pathology are stronger predictors of impairment. We evaluate whether measures of temporal lobe pathology derived from diffusion tensor imaging (DTI; *microstructural*) versus structural MRI (sMRI; *morphometric*) contribute the most to memory performances in TLE, after controlling for hippocampal volume (HCV). DTI and sMRI were performed on 26 patients with TLE and 35 controls. Verbal memory was measured with the Logical Memory subtest of the Wechsler Memory Scale–III. Hierarchical regression analyses were performed to examine unique contributions of DTI and sMRI measures to verbal memory with HCV entered in block 1. In patients, impaired recall was associated with increased mean diffusivity (MD) of multiple fiber tracts that project through the temporal lobes. In addition, increased MD of the left cortical and bilateral pericortical white matter was associated with impaired recall. After controlling for left HCV, only microstructural measures of white matter pathology contributed to verbal recall. The best predictive model included left HCV and MD of the left inferior longitudinal fasciculus (ILF) and pericortical white matter beneath the left entorhinal cortex. This model explained 60% of the

Address for correspondence: Carrie McDonald, Multimodal Imaging Laboratory, 8950 Villa La Jolla Dr, Suite C101, La Jolla, CA 92037; phone: +1 858-534-2678; fax: +1 858-534-1078; camcdonald@ucsd.edu.

variance in delayed recall and revealed that MD of the left ILF was the strongest predictor. These data reveal that white matter microstructure within the temporal lobe can be used in conjunction with left HCV to enhance the prediction of verbal memory impairment, and speak to the complementary nature of DTI and sMRI for understanding cognitive dysfunction in epilepsy and possibly other memory disorders.

Keywords

cortical thickness; diffusion tensor imaging; temporal lobe epilepsy; verbal memory; volumetric imaging

1. INTRODUCTION

Impairments in verbal episodic memory are present in approximately half of patients with chronic temporal lobe epilepsy (TLE) (Hermann, Seidenberg, Lee, Chan, & Rutecki, 2007) and a moderate correlate of this impairment is the degree of hippocampal atrophy on MRI (Alessio et al., 2006; Baxendale et al., 1998; Kilpatrick et al., 1997; Trenerry et al., 1993). However, hippocampal atrophy alone cannot explain the magnitude of memory impairments observed in TLE, leading researchers to examine the contribution of adjacent gray and white matter structures. Studies of gray matter density (i.e., voxel-based morphometry; VBM) and MRI volumetry have demonstrated the importance of both the perirhinal (Alessio et al., 2006) and entorhinal (Bonilha et al., 2007a) cortices in aspects of verbal memory. Additionally, global white matter (Hermann, Seidenberg, & Bell, 2002) and temporal lobe volumes (Lencz et al., 1992) have shown modest associations with impaired memory performances in TLE. These data support an evolving literature implicating a network of gray and white matter structures in episodic memory impairments. However, volumetric and density measurements may not detect subtle tissue changes present in patients with chronic TLE, which may limit their associations with verbal memory impairments and other cognitive morbidity.

Diffusion-weighted imaging probes the underlying microstructure of brain tissue, which could provide new insights into memory dysfunction in TLE. In particular, diffusion tensor imaging (DTI) measures the relative motility of water within a voxel (mean diffusivity; MD) and its directionality (fractional anisotropy; FA) (Concha, Beaulieu, & Gross, 2005; Wakana et al., 2007). Higher MD and lower FA values are thought to reflect microstructural tissue damage, such as demyelination and axonal injury, which can be measured within specific fiber tracts and regions of interest (ROIs) (Beaulieu, 2002). DTI studies have shown that microstructural damage to tracts projecting through the temporal lobes, including the uncinate fasciculus (UNC), inferior longitudinal fasciculus (ILF), inferior frontal occipital fasciculus (IFOF), and parahippocampal cingulum (PHC) is associated with memory impairment in TLE (Diehl et al., 2008; McDonald et al., 2008a; Yogarajah et al., 2008). Microstructural damage within medial and anterior temporal lobe ROIs has also been linked to impaired immediate and delayed memory performances, respectively (Riley et al., 2010), and there is some evidence that DTI measurements are more sensitive than white matter volumes for predicting cognitive impairments in TLE (McDonald et al., 2008a). Beyond the

deep white matter, microstructural damage can also be quantified within the cortex and the subadjacent white matter (Govindan, Asano, Juhasz, Jeong, & Chugani, 2013; Kang, Herron, Turken, & Woods, 2012; McNab et al., 2013). These pericortical diffusion measures may add value to the understanding of regional pathology in TLE since white matter proximal to a cortical region preferentially contains afferent and efferent fibers associated with that cortical region; thus, providing insight into the integrity of the region. To date, these measures have shown promise for identifying epileptogenic cortex in patients with extratemporal epilepsy (Govindan et al., 2013), as well as detecting occult cortical pathology in patients with other neurological (Liu, Young, Huang, Chen, & Wong, 2006; Turken et al., 2009) and psychiatric (Manoach et al., 2007) disorders.

Complementing advanced DTI measurements, cortical thickness and gray-white contrast can be quantified on T_1-weighted volumes point-by-point along the cortical surface (Fischl, Sereno, & Dale, 1999; Fischl et al., 2004). The addition of these advanced surface-based measurements has improved our ability to estimate total disease burden in TLE (Bernhardt et al., 2009; Lin et al., 2007; McDonald et al., 2008b; Mueller et al., 2009), as well as to detect of malformations of cortical development (Thesen et al., 2011). There is one recent study demonstrating that cortical thinning may also enhance our understanding of memory impairments in TLE (Mueller et al., 2012). However, it has not been determined whether a combination of DTI and structural MRI (sMRI) variables provides the best estimate of memory impairment in TLE. This knowledge could be very important to surgical decision-making since understanding which temporal lobe structures and tissue properties (i.e., microstructural vs morphometric) are most associated with preoperative memory in TLE may improve our ability to determine overall risk for postoperative memory decline following anterior temporal lobectomy (ATL).

In the current study, we evaluate whether microstructural (i.e., DTI: fiber tract integrity, cortical/pericortical diffusion) and/or T_1-derived/morphometric (i.e., cortical thickness, white matter volume, and gray-white contrast) measures of temporal lobe pathology improve the prediction of memory performance in TLE, after controlling for hippocampal volume (HCV). We then evaluate whether a multimodal model of these T_1-weighted sMRI and DTI metrics can increase our explanatory power. Based on our previous data, we hypothesize that although left HCV will make the strongest contribution to verbal memory performance, measures of temporal lobe white and gray matter microstructure will make independent contributions to memory performance in TLE.

2. MATERIALS AND METHODS

2.1 Participants

This study was approved by the Institutional Review Board at the University of California, San Diego (UCSD) and all participants provided informed consent according to the Declaration of Helsinki. Twenty-six patients with medically refractory TLE and 35 age- and gender-matched controls had T_1-weighted sMRI, DTI, and neuropsychological data that allowed for inclusion in the study. All patients were under evaluation for surgical treatment at the UCSD Epilepsy Center. They were diagnosed with medically refractory epilepsy by board-certified neurologists with expertise in epileptology (E.S.T and V.J.I.), according to

the criteria defined by the International League Against Epilepsy. Patients were classified into left TLE (LTLE; n=13) or right TLE (RTLE; n=13) based on seizure onsets recorded by video-EEG, seizure semiology, and neuroimaging results. Where clinically indicated, patients underwent Phase II video-EEG monitoring using 5-contact foramen ovale electrodes to exclude bilateral independent seizure onsets. Three patients in this cohort were left-handed. Intracarotid amobarbital procedure (IAP) data were available for thirteen patients. Two patients showed evidence of bilateral language representation on the IAP, whereas all other patients were left-dominant for language. Clinical MRI scans were available on all patients (i.e., T_1-weighted, T_2-weighted, and coronal FLAIR sequences with 1mm slices through the MTL). MRIs were visually inspected by a board-certified neuroradiologist for detection of mesial temporal sclerosis (MTS) and the exclusion of contralateral temporal lobe structural abnormalities. In 18 patients (11 LTLEs, 7 RTLEs), MRI findings suggested the presence of ipsilateral MTS. No patients showed evidence of contralateral MTS or extra-hippocampal pathology on clinical MRI. Three patients had a history of febrile seizures (1 LTLE, 2 RTLE). Control participants were screened for neurological or psychiatric conditions.

2.2 Procedure

2.2.1 Episodic Memory—The Logical Memory (LM) subtest from the Wechsler Memory Scale–Third Edition (WMS-III) was used to evaluate immediate (LM I) and delayed (LM II) verbal memory. This subtest measures prose recall, which has been shown to be sensitive to HCV loss (Baxendale et al., 1998; Griffith, Pyzalski, Seidenberg, & Hermann, 2004) and is among the most commonly used verbal memory measures in surgical epilepsy centers. LM I and II scaled scores were used as the dependent variable in all analyses.

2.2.2 Image Acquisition—MRIs were performed on a General Electric (GE) 1.5T EXCITE HD scanner with an 8-channel phased-array head coil. Image acquisitions included a conventional 3-plane localizer, GE calibration scan, two T_1-weighted 3D structural scans (TE=3.8ms, TR=10.7ms, flip angle=8 degrees, bandwidth=31.25 Hz/pixel, FOV=25.6 cm, matrix=192 × 256, slice thickness=1.0mm), and three diffusion-weighted sequences (total scan time = 40 minutes). Diffusion data were acquired using single-shot echo-planar imaging with isotropic 2.5 mm voxels (matrix size=96 × 96, FOV=24 cm, 47 axial slices, slice thickness=2.5 mm, partial k-space acquisition, TE=75.6 msec, TR=12.3 sec; 11 minutes total), covering the entire cerebrum and brainstem without gaps. One volume series was acquired with 51 diffusion gradient directions using a b-value of 1000 mm^2/s with an additional b=0 volume. For use in nonlinear B0 distortion correction, two additional b=0 volumes were acquired with either forward or reverse phase-encode polarity. All patients were seizure-free per self-report for a minimum of 24 hours prior to the MRI scan (Yogarajah, & Duncan, 2008).

2.2.3 Image Processing—Image files in DICOM format were transferred to a Linux workstation for further processing.

2.2.3.1 Diffusion image processing: Preprocessing of the diffusion data included correction for B_0 distortion, eddy current distortions, gradient nonlinearity distortions, and head

motion, as well as registration to the T_1-weighted structural image. For B_0 distortion correction, a reverse gradient method was used (Chang, & Fitzpatrick, 1992; Holland, Kuperman, & Dale, 2010; Morgan, Bowtell, McIntyre, & Worthington, 2004). This method provides superior accuracy and better cross-modality registration relative to the widely used field mapping approach. Displacement fields were estimated from a pair of short calibration scans with opposite phase-encode polarity. The displacement field volume was resampled and aligned with each volume of the diffusion data, accounting for estimated head motion (see below) and then used to unwarp the spatial and intensity distortions in each frame. Eddy currents were corrected with a method that uses the distortion gradients to predict the pattern of distortions across the entire set of diffusion weighted volumes (Zhuang et al., 2006). This method uses a least squares inverse and iterative conjugate gradient descent. Degrees of freedom are limited by restricting corrections to only translation and scaling in the acquisition slice plane along the phase-encode direction, avoiding spurious head rotations that are introduced by the commonly used affine registration approach. Gradient nonlinearity distortions were corrected for each frame of the diffusion data (Jovicich et al., 2006). To correct for head motion, each frame was rigidly registered to the corresponding volume synthesized from the parameters obtained through diffusion tensor fitting, accounting for variation in image contrast across diffusion orientations (Hagler et al., 2009). Between-scan motion was estimated by registering the initial b=0 (non diffusion-weighted) images of each scan. The matrix of diffusion gradient directions was adjusted for head rotation (Leemans, & Jones, 2009). For registration to the structural image, T_2-weighted b=0 images were automatically registered to the T_1-weighted scan using mutual information (Wells, Viola, Atsumi, Nakajima, & Kikinis, 1996) after coarse pre-alignment via within-modality registration to atlas brains. Diffusion images were resampled into a standard orientation with 1.875 mm isotropic resolution, matching the in-plane resolution of images produced by the scanner (note that the actual imaging resolution was 2.5 mm isotropic). To reduce the number of resampling steps, this step was combined with the between- and within-scan motion correction.

2.2.3.2 Fiber tract calculations: Fiber tract fractional anisotropy (FA) and mean diffusivity (MD) values were derived using a probabilistic diffusion tensor atlas of fiber tract locations and orientations that was developed using in-house software written in Matlab and C++ (i.e., AtlasTrack) and validated in both healthy controls and patients with TLE (Hagler et al., 2009). This atlas was constructed by manually tracing fiber tracts of 42 participants (21 healthy controls and 21 patients with TLE) with DTI Studio (John Hopkins University, Baltimore, MD) using the multiple ROI procedure described by Wakana et al. (2004). Data from this manual training set were used to create the probabalistic fiber atlas that consisted of averaged information about the locations and local orientations of the thirteen fiber tracts. Diffusion measures for the atlas-generated fibers have been shown to correlate highly with those obtained from manual tracings (average $R^2 = .98$). However, the atlas has the advantage of eliminating the time demands of manual tracings, as well as operator bias.

For each participant in this study, T_1-weighted images were used to nonlinearly register the brain to a common space, and diffusion tensor orientation estimates were compared to the atlas to obtain a map of the relative probability that a voxel belongs to a particular fiber

given the location and similarity of diffusion orientations. FreeSurfer's automated brain segmentation (Fischl et al., 2002) was used to identify and exclude voxels in the fiber tract ROIs that were primarily CSF or gray matter, independent of the DTI-derived measures of interest. Average FA and MD were calculated for each fiber tract ROI, weighted by AtlasTrack fiber probability values. The fiber probability represents a relative measure of the likelihood that a particular fiber tract occurs at a given location. It was derived from the streamline density of the manually selected fibers that were used to create the original atlas (averaged across subjects and then normalized). So that voxels with very low probability of belonging to a given fiber did not contribute to average values, a fiber probability threshold of 0.08 was used. This threshold value was empirically determined because it provided optimal correspondence in fiber volume between atlas-derived and manually traced fiber tract ROIs (see Hagler et al., 2009 for details). In the current study, this probabilistic atlas-based method was used to obtain the following right and left hemisphere fiber tracts due to their projections from the temporal lobe and previous evidence of their contribution to memory performances in TLE (Diehl et al., 2008; McDonald et al., 2008a; Yogarajah et al., 2008): fornix excluding the fimbria (FxC), PHC, UNC, ILF and IFOF (see Figure 1; top panel).

2.2.3.3 Structural MRI processing: Two T_1-weighted images were rigid body registered to each other, averaged, and reoriented into a common space, similar to alignment based on the anterior commissure-posterior commissure line. Images were corrected for non-linear warping caused by non-uniform fields created by the gradient coils (Jovicich et al., 2006). Image intensities were corrected for spatial sensitivity inhomogeneities in the 8-channel head coil by normalizing with the ratio of a body coil scan to a head coil scan.

2.2.3.4 Volumetric analysis: HCVs and white matter volumes were derived using the automated segmentation alogorithm available in Freesurfer software 5.1.0 (http://surfer.nmr.mgh.harvard.edu) (Fischl et al., 2002). Right and left HCVs were corrected for total intracranial volume.

2.2.3.5 Surface reconstruction and parcellation/Cortical Thickness: Individual T_1-weighted images were used to construct models of each participant's cortical surfaces using FreeSurfer. From this reconstructed surface, measures of cortical thickness were obtained using procedures described previously (Fischl, & Dale, 2000). Sulcal and gyral features across individual participants were aligned by morphing each participant's brain to an average spherical representation that allows for accurate matching of cortical thickness measurement locations among participants, while minimizing metric distortion. Thickness estimates were computed at each vertex (~1mm spacing) across the cortical mantle and within gyral-based ROIs (Desikan et al., 2006). Mean thickness for each ROI was calculated by averaging the cortical thickness measurements at each vertex within a given ROI. In this study, individual ROIs of interest included three lateral temporal lobe (LTL) ROIs (i.e., inferior, middle, and superior temporal) and four medial temporal lobe (MTL) ROIs (i.e., enthorhinal, parahippocampal, temporal pole, and fusiform) (Figure 1; bottom panel).

2.2.3.6 Cortical contrast: T_1-weighted intensity values were sampled on to the FreeSurfer-derived white matter/gray matter boundary at a distance of 0.2 mm along the surface normal vector, either down into the white matter or up into the gray matter. Cortical contrast at each vertex was then calculated as the difference of white and gray matter divided by their sum. White and gray matter T_1-weighted intensity values were also averaged within each FreeSurfer cortical parcellation ROI and cortical contrast for each ROI was calculated at each vertex (white matter-gray matter/(white matter+gray matter)). The use of a normalized difference metric adjusts tissue values with regards to local imaging environment as closely neighboring white and gray matter voxel intensities are expected to be similarly influenced by scanner and sequence-related noise. Right and left MTL and LTL variables were calculated from the gyral-based ROIs.

2.2.3.7 Diffusion of cortical and pericortical white matter: FreeSurfer creates anatomical labels for regions of cortical surface based on cortical folding patterns and alignment with cortical surface atlas. Each of these cortical labels are mapped back to the image volume, both within the cortical ribbon and in pericortical white matter up to a depth of 5 mm (Salat et al., 2009). These gray and white matter ROIs derived from the T1-weighted images were then resampled with nearest neighbor interpolation to the orientation and resolution of the DTI data (1.875 mm isotropic). For each of these cortical and pericortical ROIs, diffusion-derived values were averaged; average ROI values were then combined to create right and left MTL and LTL variables.

2.2.4 Statistical Analysis—Statistical analyses were conducted with SPSS Statistics 21.0 (http://www.spss.com/). First, partial correlations controlling for age were performed between variables within each MRI "set" and LM I and II subtest scores. Variable sets included (1) fiber tract FA/MD values, (2) left and right white matter volumes, and MTL/LTL values for each of the following: (3) cortical MD, (4) pericortical white matter MD, (5) cortical thickness, and (6) gray-white contrast. Bonferroni corrections were performed within each set of variables to control for Type I errors. Only variables that survived the correction were entered into the regression analyses. Hierarchical regression analyses were then performed with age and left HCV in block 1, each significant MRI variable that survived correction in block 2, and LM scores as the dependent variables. Post-hoc stepwise regressions were performed to evaluate independent contributions of MTL/LTL subregion ROIs to LM scores when the overall lobar value was a significant contributor. A final multiparameter regression was performed that included all predictor variables that showed a significant R^2 Δ in block 2. This analysis allowed us to estimate what linear combination of MRI variables best explained LM scores.

3. RESULTS

Table 1 displays the demographic, disease-related and LM variables for the patient and control groups. There were no statistically significant differences among the controls, LTLEs, or RTLEs in age, or years of education ($F[2,71] = .04$, $p > .10$, $F[2,70] = 2.99$, $p > .05$, respectively). The distribution of gender across the three groups was comparable ($\chi^2[2] = .34$, $p = .85$). There were no statistically significant differences between the two patient groups in disease duration ($t = -.94$, $p > .10$), age at seizure onset ($t = .85$, $p > .10$), or the

number of patients with MTS ($\chi^2[1] = 1.93$, $p = .16$). The volume of the ipsilateral hippocampus did not differ between the two patient groups, although there was a trend for those with LTLE to have smaller ipsilateral HCVs ($t[34] = -1.99$, $p = .054$). Both patient groups' ipsilateral HCVs were smaller when compared to the corresponding side of the controls HCVs ($t[52] = 5.82$, $p = .001$, and $t[52] = 2.58$, $p = .02$, LTLE and RTLE, respectively), but their contralateral HCVs were not statistically different from the controls ($t[52] = .916$, $p > .10$, and $t[52] = -.32$, $p > .10$, LTLE and RTLE, respectively).

3.1 LM scores

There were significant group differences in LM I [$F(2, 60) = 12.4$, $p < .001$] and LM II [$F(2,60) = 21.7$, $p < .001$] scaled score performances. Post-hoc analyses revealed that for both subtests, patients with LTLE and RTLE performed more poorly than controls, and patients with LTLE performed more poorly than those with RTLE (p-values < .05). Due to the sizable number of patients impaired (i.e., 1 standard deviation or more below average) in both groups (LM I; LTLE = 62%, RTLE = 31% and LM II; LTLE = 69% and RTLE = 36%), patients with RTLE and LTLE were combined in the correlation and regression analyses. However, scatterplots showing subgroup correlations can be seen in Figure 2 and the supplementary material.

There were no significant correlations between LMI or LM II scores and any of the sMRI or diffusion variables in healthy controls, after correcting for age. Therefore, all subsequent analyses were performed with patients only.

3.2 HCV

Smaller left HCV was associated with poorer LM I (r = .55) and LM II (r = .57) scores. Right HCV was not associated with either LM I or LM II scores. Therefore, all subsequent analyses were performed using the left HCV in the first block of the multiple regression analyses.

3.3 Fiber tract FA/MD

Fiber tract FA/MD values were highly intercorrelated (Pearson *rhos* = .52–.77). Therefore, we elected to only include MD values in the analysis based on our previous results (McDonald et al., 2008a) and our current analyses demonstrating higher correlations between fiber tract MD and cognitive variables (see Table 2). Partial correlations demonstrated that after correcting for age (Bonferroni-corrected p-values < .005), higher MD of the left ILF was associated with lower LM I scores in patients with TLE. Higher MD of the left PHC and UNC and bilateral ILF and IFOF were associated with lower LM II scores in patients with TLE. Hierarchical regression analyses demonstrated that after covarying out the effects of age and left HCV, MD of the left ILF only approached significance for LM I ($R^2 \Delta = .10$, $p = .07$); whereas, MD of the left UNC ($R^2 \Delta = .19$, $p = .008$), left ILF ($R^2 \Delta = .25$, $p = .001$), left IFOF ($R^2 \Delta = .20$, $p = .006$), right ILF ($R^2 \Delta = .24$, $p = .002$), and right IFOF ($R^2 \Delta = .22$, $p = .003$) all remained significant contributors to LM II score. Stepwise regression indicated that MD of the left ILF uniquely contributed to LM II scores when controlling for HCV. Together, left HCV and MD of the left ILF explained 59% of the variance in LM II score.

3.4 Pericortical white matter MD

Partial correlations (Bonferroni-corrected p-values < .0125) demonstrated that higher MD of the left and right MTL and left LTL pericortical white matter was associated with poorer LM II scores only. Hierarchical regression analysis demonstrated that all three regional MD values were significant predictors after controlling for HCV (left MTL R^2 Δ = .15, p = .020; left LTL R^2 Δ = .20, p = .006; right MTL R^2 Δ = .18, p = .006). Subregional analysis indicated that within the left MTL, MD of the left entorhinal white matter was the best predictor (R^2 Δ = .18, p = .009). Within the left LTL, MD of the left inferior temporal pericortical white matter was the best predictor (R^2 Δ = .22, p = .004). Within the right LTL, MD of the right superior temporal gyrus was the best predictor (R^2 Δ = .21, p = .005). Together with left HCV, these variables explained 57% of the variance in LM II scores.

3.5 Cortical MD

Partial correlations (i.e., Bonferroni-corrected p-values < .0125) demonstrated that higher MD of the left LTL was associated with poorer LM II scores only. However, this region was not a significant predictor after controlling for HCV.

3.6 Cortical thickness, gray-white contrast, and white matter volumes

There were no significant partial correlations between right or left MTL/LTL cortical thickness or gray-white contrast measurements and LM I or LM II scores after controlling for age. In addition, white matter volumes did not correlate with either LM I or LM II scores. Therefore, no hierarchical regression analyses were performed for these variables.

3.7 Multiparameter regression

A multiparameter hierarchical regression analysis was performed that included all unique predictor variables across sets. This model included age and left HCV (block 1), and MD of the left ILF, left entorhinal, left inferior temporal, and right superior temporal pericortical white matter (block 2). Together, these five predictor variables explained 61% of the variance in LM II score (R^2 Δ = .61, p = .002). Regression coefficients demonstrated that left HCV (*b* = .24), MD of the left ILF (*b* = −.54) and MD of the left entorhinal pericortical white matter (*b* = −.21) accounted for most of the variance (see Figure 2), explaining 60% of the variance in LM II scores. Stepwise analysis demonstrated that MD of the left ILF was the only unique predictor. In fact, MD of the left ILF was a stronger predictor of memory than left HCV. Whereas left HCV explained 33% of the variance in LM II scores, MD of the left ILF explained 48% of the variance. In a final analysis, FA of each significant region was added to the regression model (block 3) to determine whether FA would contribute additional variance. None of the cortical/pericortical or tractography-based FA measures added to the prediction of LMII scores beyond what was explained by HCV and MD measurements.

3.8 Relationship with seizure-related variables

In order to determine whether seizure-related variables would contribute additional variance to LM I or II scores, age of seizure onset, disease duration, and seizure frequency were each

entered into separate regression as the sole predictor in block 2. None of these variables added to the estimation of LM scores after controlling for age and HCV.

3.9 Relationship to post-operative memory decline

Thirteen of the patients in this study underwent unilateral ATL and are seizure-free. Of these patients, 9 have received one-year postoperative memory testing (5 RTLE and 4 LTLE). Post-hoc analyses based on this postsurgical cohort revealed stable or improved LM II scores in all 5 patients with RTLE. Conversely, 2 patients with LTLE showed postoperative memory decline, whereas the other 2 patients showed mild improvements in verbal memory (see Figure 3). As can be seen, the two patients who showed a decline in verbal memory had lower preoperative MD of the left ILF and lower MD of the left entorhinal white matter compared to the two patients who showed mild improvements.

4. DISCUSSION

Hippocampal atrophy is the most commonly used MRI measure for estimating the risk for postoperative memory decline in patients with TLE. This is despite years of research describing the importance of other MTL and LTL structures to memory [for recent reviews, see (Bell, Lin, Seidenberg, & Hermann, 2011; Hermann, Lin, Jones, & Seidenberg, 2009; McDonald, 2008)]. With new, advanced MRI measures more readily available and easier to integrate into clinical practice, we evaluated whether these newer measurements could enhance the prediction of memory impairments in TLE. Here, we demonstrate that combined data from sMRI and DTI can explain well over half of the variance in delayed verbal recall performances. To our knowledge, this exceeds estimates obtained from previous studies that have used only HCV (Baxendale et al., 1998) or from studies that have included HCV along with volumes (Alessio et al., 2006), density (Bonilha et al., 2007a) or metabolism (Griffith et al., 2004; Weintrob, Saling, Berkovic, Berlangieri, & Reutens, 2002) of other temporal lobe structures. Specifically, we found that microstructural integrity of the left ILF and left entorhinal white matter coupled with left HCV explained 60% of the variance in delayed verbal memory scores. This suggests that white matter compromise within the left temporal lobe is an independent predictor of memory impairment in TLE that could serve as an important MRI risk factor for postoperative memory decline.

The finding that white matter microstructure within the temporal lobe is related to memory performances is not itself novel. Both research from our lab (McDonald et al., 2008a) and from others (Diehl et al., 2008; Riley et al., 2010) has demonstrated this association in TLE. Nevertheless, our findings are unique in two ways. First, we demonstrate that measures of temporal lobe white matter microstructure provide the best and only *unique* information for estimating verbal memory performances. That is, both MD of the left ILF and MD of the white matter underlying the entorhinal cortex emerged as strong predictors after controlling for HCV, whereas this was not the case with any of our measures of cortical pathology (i.e., cortical MD, thickness, or contrast). The ILF is a long association fiber tract that courses through the temporal lobes, projecting from the temporal pole and superior temporal sulcus, with caudal branches extending vertically into inferior parietal lobe and horizontally into inferior temporal and fusiform regions (Schmahmann et al., 2007). This fiber tract has been

implicated in memory performances in patients with TLE (McDonald et al., 2008a) as well as in normal age-related memory decline (Lockhart et al., 2012; Sasson, Doniger, Pasternak, Tarrasch, & Assaf, 2013). However, the ILF does not include more peripheral white matter that is known to be important to memory functions. Using pericortical diffusion measures, we found that microstructure of the white matter abutting the entorhinal cortex was also an important and unique contributor. This peripheral white matter likely includes fibers from the perforant path that provides a connectional route from the entorhinal cortex to all subfields of the hippocampus and has been implicated in memory retention (Vago, Bevan, & Kesner, 2007). The importance of these white matter pathways to memory underscores the need to take a broad, network-based approach to understanding memory in TLE—one that considers not only the hippocampus, but also its frontal, MTL, and LTL projections.

A second novel and related finding is that aside from left HCV, only *microstructural* measures of temporal lobe pathology contributed to memory function, whereas T_1-derived estimates of pathology (i.e., reductions in gray-white contrast, thickness, and white matter volume) did not make a significant contribution. Specifically, increased diffusion within the left LTL cortex was associated with verbal memory impairment, but cortical microstructure was not independent of HCV. This may indicate that subtle damage to the temporal lobe neocortex is tightly coupled to HCV loss, whereas loss of white matter integrity is at least partially independent of this HCV-cortical pathology (Concha, Beaulieu, Collins, & Gross, 2009). It is of note that one previous study described significant associations between regional cortical thinning and verbal memory impairment that differed for patients with and without MTS (Mueller et al., 2009). Mueller *et al.* combined patients and controls in the correlational analysis to broaden the range of values since the correlations did not reach statistical significance when only patients were included. Thus, it is possible that with a broader range of scores or more lenient statistical threshold, associations would have emerged in our data between regional cortical thinning and memory impairment. Our data do not preclude these associations. Rather, we conclude that microstructural measures are merely more *sensitive* correlates of memory impairment than those derived from T_1-weighted data. Although data on cortical diffusion in epilepsy is lacking [but see (Govindan et al., 2013)], these findings could have important implications for the utility of DTI-derived measures of cortical and subcortical microstructure for estimating memory dysfunction and other cognitive morbidity in TLE and related neurological disorders.

Verbal memory is a multifaceted domain whose different components have overlapping, but not identical, neurobiological substrates (Saling, 2009). In this study, we focus on the contribution of MRI measures to a specific component of verbal memory, i.e., *prose* recall. This type of verbal recall has shown moderate correlations with HCV loss (Baxendale et al., 1998; Griffith et al., 2004), but may rely more on extrahippocampal regions than other types of memory tasks. As described by Saling (Saling, 2009), LM and similar prose recall tasks are replete with semantic content and complex syntactical structure, and these attributes depend on extrahippocampal structures to a greater degree than tasks without such semantic linkages (i.e., *unrelated* paired-associate learning). That is, whereas forming new associations among unrelated items is highly dependent on the hippocampus, prose recall is less so. Although our data would suggest that both the left hippocampus and temporal lobe

white matter make important contributions to prose recall, integrity of temporal lobe white matter made a stronger contribution. This finding is commensurate with the idea that the hippocampus is not the *most* important structure in prose recall and we raise the possibility that the underlying white matter connections, rather than just temporal neocortex per se, is a highly important and often overlooked contributor. It is of note that the hippocampal vs extrahippocampal temporal lobe specialization described above is largely based on verbal memory outcomes following temporal lobe resections sparing vs not sparing the hippocampus. That is, prose recall and other tasks with a semantic component decline following en bloc resections, whereas they do not decline following selective amygdalohippocampectomy (Helmstaedter, Grunwald, Lehnertz, Gleissner, & Elger, 1997; Saling et al., 2002). Given these data, it is likely that the hippocampus would have made the strongest contribution to verbal memory performance if we had evaluated verbal associative learning and recall. Thus, our findings speak to the contribution of various MRI measures to prose recall specifically and whether this is true of other forms of verbal recall requires further investigation. Furthermore, the finding that both immediate and delayed recall of prose passages was associated with left HCV and temporal lobe microstructure is not surprising. The hippocampus and other temporal lobe regions are known to be important for both the learning and retention of information, and verbal learning requires linguistic skills that are heavily dependent on left temporal cortex (Helmstaedter et al., 1997; Saling, 2009). For this reason, we might have anticipated an association between left LTL damage and LM I impairment. Although there were trends in our data to support this notion, we found broader and more robust associations with LM II. Although patients with left and right TLE are often impaired on LM I and II (Castro et al., 2013; Saling, 2009), delayed verbal recall was of most concern in this study given the emphasis on delayed memory in preoperative neuropsychological evaluations. It is of note that our findings are in line with previous research indicating that the initial acquisition of verbal information is highly left lateralized, whereas retention of verbal information relies on the integrity of both left and right temporal lobe regions (Saling, 2009). We extend these findings to reveal which regions and MRI parameters provide the best information for predicting verbal memory impairment in TLE.

There are several limitations of this study that should be discussed. First, we limited our analysis to temporal lobe structures and fiber tracts that project through the temporal lobes. It is well known that extratemporal regions contribute to verbal memory performances and there is some evidence that prefrontal and cingulate regions add unique variance to the prediction of memory performance in TLE (Bonilha et al., 2007b; Mueller et al., 2012). Although it would be of interest to take a whole brain approach to analyzing our multimodal data, the number of predictor variables would have presented a statistical challenge. Thus, we decided to take a hypothesis driven approach, using strict Bonferroni corrections and focusing on those regions and fiber tracts that are (1) *most* implicated in verbal memory performance and (2) *directly* impacted by temporal lobe resections. The second point deserves elaboration in that the primary clinical utility of defining regional contributions to memory is for understanding what the surgical removal of specific structures may be on memory performance. However, this does not take into account the effects of deafferentiation, or *indirect*, contributions to memory. Such data will be borne out of complex network modeling that integrates multimodal data. To date, most network modeling

has focused on data from only one modality (Bernhardt, Hong, Bernasconi, & Bernasconi, 2013), whereas the purpose of our paper was to integrate data across modalities and sequences (i.e., sMRI and DTI). Efforts to examine the added contributions of functional MRI data are underway and should prove beneficial for capturing the variance associated with reorganization of memory function. Second, we examined independent contributions of different brain regions and MRI measures to memory performance to better appreciate how much these regions/measures add to HCV. However, multicollinearity among some of the predictor variables was high, which may have resulted in our removing otherwise important predictors from our stepwise regression analyses. Other multivariate approaches, including principal components analysis, have been proposed that take advantage of multicollinearity within data sets and extract sets of latent variables (i.e., components) that can be used as predictors. This data reduction method has been used to form latent neuropsychological components for predicting postoperative memory decline (St-Laurent et al., 2013), and to facilitate EEG source localization in TLE (Stern et al., 2009). However, it is largely data-driven and atheoretical and we choose to use a more hypothesis-driven approach in our study. Third, we combined patients with LTLE and RTLE in our group analysis given that both groups showed the same general pattern of verbal memory-MRI associations, following along a similar regression line (see Figure 2 and the Supplemental Figure). However, it is important to note that the associations were somewhat stronger in patients with LTLE, who also had smaller left HCVs and a greater number of patients with MTS. Therefore, although the same MRI variables appear to be associated with verbal memory impairments in patients with RTLE and LTLE, subgroup analyses in a larger patient cohort could reveal unique associations that we were not able to detect given the limitations of our sample size. Fourth, some of the newer measurements described in this study (i.e., cortical and pericortical diffusion measures) are receiving increased attention in the neuroimaging literature given their proposed ability to provide insight into the cytoarchitectonic organization of the human cortex and add to the morphological information provided by T_1-weighted images (Behrens, Jenkinson, Robson, Smith, & Johansen-Berg, 2006). However, there are methodological issues related to these measurements (Kang et al., 2012). In particular, given the thin and variable nature of the cortex, and the diffusion imaging voxel size of 2.5 mm, MD of cortical regions is likely to be contaminated to some degree by partial voluming with CSF, and pericortical white matter ROIs may be affected by partial voluming with adjacent gray matter. Because of this, results from the pericortical, and especially cortical ROIs should be considered tentative, pending higher resolution diffusion imaging. The most likely effect of CSF contamination would be to increase variance and reduce the likelihood of significant associations; this is a potential explanation for non-significant results for cortical ROIs. As discussed above, we evaluated only one type of memory, i.e., verbal recall of prose. Therefore, our interpretations are limited in scope. However, we wished to focus our paper on a very common type of memory impairment that is frequently impaired in patients with LTLE and RTLE, using one of the most commonly administered verbal memory tests. This allowed us to test our multimodal data on a single question using a manageable number of variables. Whether our findings regarding the importance of white matter microstructure will extend to other types of memory or cognitive co-morbidity will require further investigation.

5. CONCLUSION

Our data reveal that microstructural measures of temporal lobe pathology are more sensitive than morphometric measures for predicting verbal memory impairment in patients with TLE, and that white matter microstructure provides unique information above and beyond HCV loss. These data speak to the complementary nature of DTI and sMRI for understanding cognitive dysfunction in TLE that could extend to patients with a range of memory disorders.

Supplementary Material

Refer to Web version on PubMed Central for supplementary material.

Acknowledgments

We wish to thank Holly M. Girard for assistance in data collection and processing and Richard Loi for assistance with figures. We also wish to thank the patients of the UCSD Epilepsy Center who devoted their time and clinical data for research purposes.

FUNDING

This work was supported by the National Institute of Neurological Disorders and Stroke (R01NS065838 to CRM). The NIH had no role in the study design; in the collection, analysis and interpretation of data; in the writing of the report; or in the decision to submit the article for publication.

Abbreviations

ATL	anterior temoral lobectomy
DTI	diffusion tensor imaging
FA	fractional anisotropy
HCV	hippocampal volume
IFOF	inferior fronto-occipital fasciculus
ILF	inferior longitudinal fasciculus
LTL	lateral temporal lobe
LTLE	left temporal lobe epilepsy
LM	Logical Memory
MD	mean diffusivity
MTL	medial temporal lobe
MTS	mesial temporal sclerosis
PHC	parahippocampal cingulum
ROIs	regions of interest
RTLE	right temporal lobe epilepty
TLE	temporal lobe epilepsy

UNC	uncinate fasciculus
sMRI	volumetric MRI
VBM	voxel-based morphometry

References

Alessio A, Bonilha L, Rorden C, Kobayashi E, Min LL, Damasceno BP, Cendes F. Memory and language impairments and their relationships to hippocampal and perirhinal cortex damage in patients with medial temporal lobe epilepsy. Epilepsy Behav. 2006; 8(3):593–600. [PubMed: 16517214]

Baxendale SA, van Paesschen W, Thompson PJ, Connelly A, Duncan JS, Harkness WF, Shorvon SD. The relationship between quantitative MRI and neuropsychological functioning in temporal lobe epilepsy. Epilepsia. 1998; 39(2):158–166. [PubMed: 9577995]

Beaulieu C. The basis of anisotropic water diffusion in the nervous system - a technical review. NMR Biomed. 2002; 15(7–8):435–455. [PubMed: 12489094]

Behrens TE, Jenkinson M, Robson MD, Smith SM, Johansen-Berg H. A consistent relationship between local white matter architecture and functional specialisation in medial frontal cortex. Neuroimage. 2006; 30(1):220–227. [PubMed: 16271482]

Bell B, Lin JJ, Seidenberg M, Hermann B. The neurobiology of cognitive disorders in temporal lobe epilepsy. Nat Rev Neurol. 2011; 7(3):154–164. [PubMed: 21304484]

Bernhardt BC, Hong S, Bernasconi A, Bernasconi N. Imaging structural and functional brain networks in temporal lobe epilepsy. Front Hum Neurosci. 2013; 7:624. [PubMed: 24098281]

Bernhardt BC, Worsley KJ, Kim H, Evans AC, Bernasconi A, Bernasconi N. Longitudinal and cross-sectional analysis of atrophy in pharmacoresistant temporal lobe epilepsy. Neurology. 2009; 72(20): 1747–1754. [PubMed: 19246420]

Bonilha L, Alessio A, Rorden C, Baylis G, Damasceno BP, Min LL, Cendes F. Extrahippocampal gray matter atrophy and memory impairment in patients with medial temporal lobe epilepsy. Hum Brain Mapp. 2007a; 28(12):1376–1390. [PubMed: 17370345]

Bonilha L, Rorden C, Halford JJ, Eckert M, Appenzeller S, Cendes F, Li LM. Asymmetrical extra-hippocampal grey matter loss related to hippocampal atrophy in patients with medial temporal lobe epilepsy. J Neurol Neurosurg Psychiatry. 2007b; 78(3):286–294. [PubMed: 17012334]

Castro LH, Silva LC, Adda CC, Banaskiwitz NH, Xavier AB, Jorge CL, Nitrini R. Low prevalence but high specificity of material-specific memory impairment in epilepsy associated with hippocampal sclerosis. Epilepsia. 2013; 54(10):1735–1742. [PubMed: 23980806]

Chang H, Fitzpatrick JM. A technique for accurate magnetic resonance imaging in the presence of field inhomogeneities. IEEE Trans Med Imaging. 1992; 11(3):319–329. [PubMed: 18222873]

Concha L, Beaulieu C, Collins DL, Gross DW. White-matter diffusion abnormalities in temporal-lobe epilepsy with and without mesial temporal sclerosis. J Neurol Neurosurg Psychiatry. 2009; 80(3): 312–319. [PubMed: 18977826]

Concha L, Beaulieu C, Gross DW. Bilateral limbic diffusion abnormalities in unilateral temporal lobe epilepsy. Ann Neurol. 2005; 57(2):188–196. [PubMed: 15562425]

Desikan RS, Segonne F, Fischl B, Quinn BT, Dickerson BC, Blacker D, Killiany RJ. An automated labeling system for subdividing the human cerebral cortex on MRI scans into gyral based regions of interest. Neuroimage. 2006; 31(3):968–980. [PubMed: 16530430]

Diehl B, Busch RM, Duncan JS, Piao Z, Tkach J, Luders HO. Abnormalities in diffusion tensor imaging of the uncinate fasciculus relate to reduced memory in temporal lobe epilepsy. Epilepsia. 2008; 49(8):1409–1418. [PubMed: 18397294]

Fischl B, Dale AM. Measuring the thickness of the human cerebral cortex from magnetic resonance images. Proc Natl Acad Sci U S A. 2000; 97(20):11050–11055. [PubMed: 10984517]

Fischl B, Salat DH, Busa E, Albert M, Dieterich M, Haselgrove C, Dale AM. Whole brain segmentation: automated labeling of neuroanatomical structures in the human brain. Neuron. 2002; 33(3):341–355. [PubMed: 11832223]

Fischl B, Sereno MI, Dale AM. Cortical surface-based analysis. II: Inflation, flattening, and a surface-based coordinate system. Neuroimage. 1999; 9(2):195–207. [PubMed: 9931269]

Fischl B, van der Kouwe A, Destrieux C, Halgren E, Segonne F, Salat DH, Dale AM. Automatically parcellating the human cerebral cortex. Cereb Cortex. 2004; 14(1):11–22. [PubMed: 14654453]

Govindan RM, Asano E, Juhasz C, Jeong JW, Chugani HT. Surface-based laminar analysis of diffusion abnormalities in cortical and white matter layers in neocortical epilepsy. Epilepsia. 2013; 54(4):667–677. [PubMed: 23448199]

Griffith HR, Pyzalski RW, Seidenberg M, Hermann BP. Memory relationships between MRI volumes and resting PET metabolism of medial temporal lobe structures. Epilepsy Behav. 2004; 5(5):669–676. [PubMed: 15380118]

Hagler DJ Jr, Ahmadi ME, Kuperman J, Holland D, McDonald CR, Halgren E, Dale AM. Automated white-matter tractography using a probabilistic diffusion tensor atlas: Application to temporal lobe epilepsy. Hum Brain Mapp. 2009; 30(5):1535–1547. [PubMed: 18671230]

Helmstaedter C, Grunwald T, Lehnertz K, Gleissner U, Elger CE. Differential involvement of left temporolateral and temporomesial structures in verbal declarative learning and memory: evidence from temporal lobe epilepsy. Brain Cogn. 1997; 35(1):110–131. [PubMed: 9339305]

Hermann BP, Lin JJ, Jones JE, Seidenberg M. The emerging architecture of neuropsychological impairment in epilepsy. Neurol Clin. 2009; 27(4):881–907. [PubMed: 19853214]

Hermann BP, Seidenberg M, Bell B. The neurodevelopmental impact of childhood onset temporal lobe epilepsy on brain structure and function and the risk of progressive cognitive effects. Prog Brain Res. 2002; 135:429–438. [PubMed: 12143361]

Hermann BP, Seidenberg M, Lee EJ, Chan F, Rutecki P. Cognitive phenotypes in temporal lobe epilepsy. J Int Neuropsychol Soc. 2007; 13(1):12–20. [PubMed: 17166299]

Holland D, Kuperman JM, Dale AM. Efficient correction of inhomogeneous static magnetic field-induced distortion in Echo Planar Imaging. Neuroimage. 2010; 50(1):175–183. [PubMed: 19944768]

Jovicich J, Czanner S, Greve D, Haley E, van der Kouwe A, Gollub R, Dale A. Reliability in multi-site structural MRI studies: effects of gradient non-linearity correction on phantom and human data. Neuroimage. 2006; 30(2):436–443. [PubMed: 16300968]

Kang X, Herron TJ, Turken AU, Woods DL. Diffusion properties of cortical and pericortical tissue: regional variations, reliability and methodological issues. Magn Reson Imaging. 2012; 30(8): 1111–1122. [PubMed: 22698767]

Kilpatrick C, Murrie V, Cook M, Andrewes D, Desmond P, Hopper J. Degree of left hippocampal atrophy correlates with severity of neuropsychological deficits. Seizure. 1997; 6(3):213–218. [PubMed: 9203250]

Leemans A, Jones DK. The B-matrix must be rotated when correcting for subject motion in DTI data. Magn Reson Med. 2009; 61(6):1336–1349. [PubMed: 19319973]

Lencz T, McCarthy G, Bronen RA, Scott TM, Inserni JA, Sass KJ, Spencer DD. Quantitative magnetic resonance imaging in temporal lobe epilepsy: relationship to neuropathology and neuropsychological function. Ann Neurol. 1992; 31(6):629–637. [PubMed: 1514774]

Lin JJ, Salamon N, Lee AD, Dutton RA, Geaga JA, Hayashi KM, Thompson PM. Reduced Neocortical Thickness and Complexity Mapped in Mesial Temporal Lobe Epilepsy with Hippocampal Sclerosis. Cereb Cortex. 2007; 17(9):2007–2018. [PubMed: 17088374]

Liu T, Young G, Huang L, Chen NK, Wong ST. 76-space analysis of grey matter diffusivity: methods and applications. Neuroimage. 2006; 31(1):51–65. [PubMed: 16434215]

Lockhart SN, Mayda AB, Roach AE, Fletcher E, Carmichael O, Maillard P, Decarli C. Episodic memory function is associated with multiple measures of white matter integrity in cognitive aging. Front Hum Neurosci. 2012; 6:56. [PubMed: 22438841]

Manoach DS, Ketwaroo GA, Polli FE, Thakkar KN, Barton JJ, Goff DC, Tuch DS. Reduced microstructural integrity of the white matter underlying anterior cingulate cortex is associated with

increased saccadic latency in schizophrenia. Neuroimage. 2007; 37(2):599–610. [PubMed: 17590354]

McDonald CR. The use of neuroimaging to study behavior in patients with epilepsy. Epilepsy Behav. 2008; 12(4):600–611. [PubMed: 18078790]

McDonald CR, Ahmadi ME, Hagler DJ, Tecoma ES, Iragui VJ, Gharapetian L, Halgren E. Diffusion tensor imaging correlates of memory and language impairments in temporal lobe epilepsy. Neurology. 2008a; 71(23):1869–1876. [PubMed: 18946001]

McDonald CR, Hagler DJ Jr, Ahmadi ME, Tecoma E, Iragui V, Gharapetian L, Halgren E. Regional neocortical thinning in mesial temporal lobe epilepsy. Epilepsia. 2008b; 49(5):794–803. [PubMed: 18266751]

McNab JA, Polimeni JR, Wang R, Augustinack JC, Fujimoto K, Stevens A, Wald LL. Surface based analysis of diffusion orientation for identifying architectonic domains in the in vivo human cortex. Neuroimage. 2013; 69:87–100. [PubMed: 23247190]

Morgan PS, Bowtell RW, McIntyre DJ, Worthington BS. Correction of spatial distortion in EPI due to inhomogeneous static magnetic fields using the reversed gradient method. J Magn Reson Imaging. 2004; 19(4):499–507. [PubMed: 15065175]

Mueller SG, Laxer KD, Barakos J, Cheong I, Garcia P, Weiner MW. Widespread neocortical abnormalities in temporal lobe epilepsy with and without mesial sclerosis. Neuroimage. 2009; 46(2):353–359. [PubMed: 19249372]

Mueller SG, Laxer KD, Scanlon C, Garcia P, McMullen WJ, Loring DW, Weiner MW. Different structural correlates for verbal memory impairment in temporal lobe epilepsy with and without mesial temporal lobe sclerosis. Hum Brain Mapp. 2012; 33(2):489–499. [PubMed: 21438080]

Riley JD, Franklin DL, Choi V, Kim RC, Binder DK, Cramer SC, Lin JJ. Altered white matter integrity in temporal lobe epilepsy: association with cognitive and clinical profiles. Epilepsia. 2010; 51(4):536–545. [PubMed: 20132296]

Salat DH, Greve DN, Pacheco JL, Quinn BT, Helmer KG, Buckner RL, Fischl B. Regional white matter volume differences in nondemented aging and Alzheimer's disease. Neuroimage. 2009; 44(4):1247–1258. [PubMed: 19027860]

Saling MM. Verbal memory in mesial temporal lobe epilepsy: beyond material specificity. Brain. 2009; 132(Pt 3):570–582. [PubMed: 19251757]

Saling, MM.; O'Shea, MF.; Weintrob, DL.; Wood, AG.; Reutens, DC.; Berkovic, SF. Medial and lateral contributions to verbal memory: evidence from temporal lobe epilepsy. In: Yamadori, A.; Kawashima, R.; Fujii, T.; Suzuki, K., editors. Frontiers of memory. Sendai: Tohoku University Press; 2002. p. 151-158.

Sasson E, Doniger GM, Pasternak O, Tarrasch R, Assaf Y. White matter correlates of cognitive domains in normal aging with diffusion tensor imaging. Front Neurosci. 2013; 7:32. [PubMed: 23493587]

Schmahmann JD, Pandya DN, Wang R, Dai G, D'Arceuil HE, de Crespigny AJ, Wedeen VJ. Association fibre pathways of the brain: parallel observations from diffusion spectrum imaging and autoradiography. Brain. 2007; 130(Pt 3):630–653. [PubMed: 17293361]

St-Laurent M, McCormick C, Cohn M, Misic B, Giannoylis I, McAndrews MP. Using multivariate data reduction to predict postsurgery memory decline in patients with mesial temporal lobe epilepsy. Epilepsy Behav. 2013

Stern Y, Neufeld MY, Kipervasser S, Zilberstein A, Fried I, Teicher M, Adi-Japha E. Source localization of temporal lobe epilepsy using PCA-LORETA analysis on ictal EEG recordings. J Clin Neurophysiol. 2009; 26(2):109–116. [PubMed: 19279504]

Thesen T, Quinn BT, Carlson C, Devinsky O, Dubois J, McDonald CR, Kuzniecky R. Detection of epileptogenic cortical malformations with surfacebased MRI morphometry. PLoS One. 2011; 6(2):e16430. [PubMed: 21326599]

Trenerry MR, Jack CR Jr, Ivnik RJ, Sharbrough FW, Cascino GD, Hirschorn KA, Meyer FB. MRI hippocampal volumes and memory function before and after temporal lobectomy. Neurology. 1993; 43(9):1800–1805. [PubMed: 8414035]

Turken AU, Herron TJ, Kang X, O'Connor LE, Sorenson DJ, Baldo JV, Woods DL. Multimodal surface-based morphometry reveals diffuse cortical atrophy in traumatic brain injury. BMC Med Imaging. 2009; 9:20. [PubMed: 20043859]

Vago DR, Bevan A, Kesner RP. The role of the direct perforant path input to the CA1 subregion of the dorsal hippocampus in memory retention and retrieval. Hippocampus. 2007; 17(10):977–987. [PubMed: 17604347]

Wakana S, Caprihan A, Panzenboeck MM, Fallon JH, Perry M, Gollub RL, Mori S. Reproducibility of quantitative tractography methods applied to cerebral white matter. Neuroimage. 2007; 36(3):630–644. [PubMed: 17481925]

Weintrob DL, Saling MM, Berkovic SF, Berlangieri SU, Reutens DC. Verbal memory in left temporal lobe epilepsy: evidence for task-related localization. Ann Neurol. 2002; 51(4):442–447. [PubMed: 11921050]

Wells WM 3rd, Viola P, Atsumi H, Nakajima S, Kikinis R. Multi-modal volume registration by maximization of mutual information. Med Image Anal. 1996; 1(1):35–51. [PubMed: 9873920]

Yogarajah M, Duncan JS. Diffusion-based magnetic resonance imaging and tractography in epilepsy. Epilepsia. 2008; 49(2):189–200. [PubMed: 17941849]

Yogarajah M, Powell HW, Parker GJ, Alexander DC, Thompson PJ, Symms MR, Duncan JS. Tractography of the parahippocampal gyrus and material specific memory impairment in unilateral temporal lobe epilepsy. Neuroimage. 2008; 40(4):1755–1764. [PubMed: 18314352]

Zhuang J, Hrabe J, Kangarlu A, Xu D, Bansal R, Branch CA, Peterson BS. Correction of eddy-current distortions in diffusion tensor images using the known directions and strengths of diffusion gradients. J Magn Reson Imaging. 2006; 24(5):1188–1193. [PubMed: 17024663]

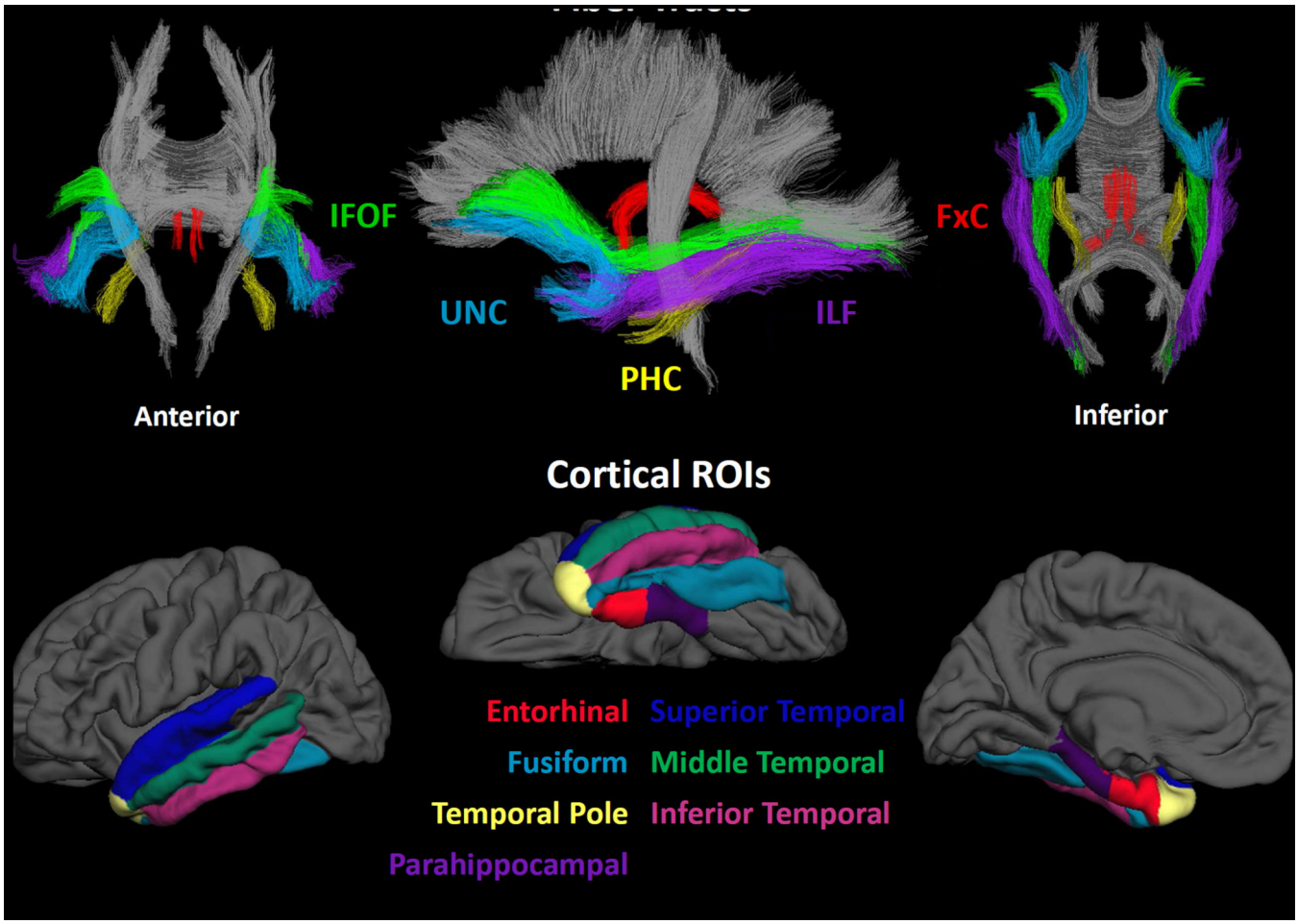

Figure 1.
Fiber tracts and temporal lobe regions of interest (ROIs)

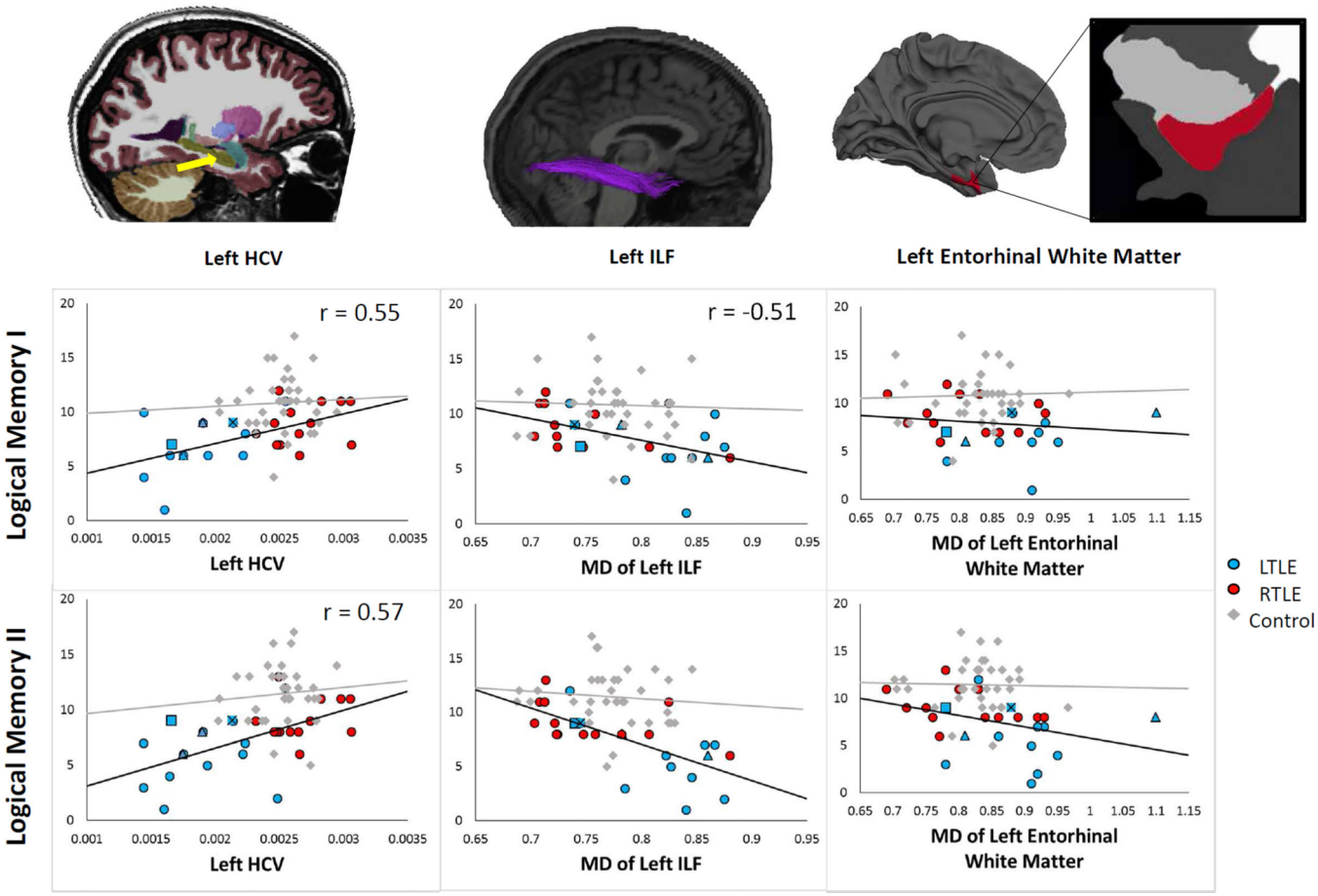

Figure 2.

Scatterplots depicting the relationship between left HCV (left), MD of the left ILF (middle) and MD of the pericortical entorhinal white matter (right) with LM I and LM II scores for patients and controls. Magnification of the left entorhinal white matter shows the distance below the cortical surface in which the white matter was sampled. Left handed patients are coded as triangles, patients who have bilateral language dominance according to the IAP are coded as squares, and one patient who is both left handed had bilateral language dominance is coded as a square with an X in the middle.

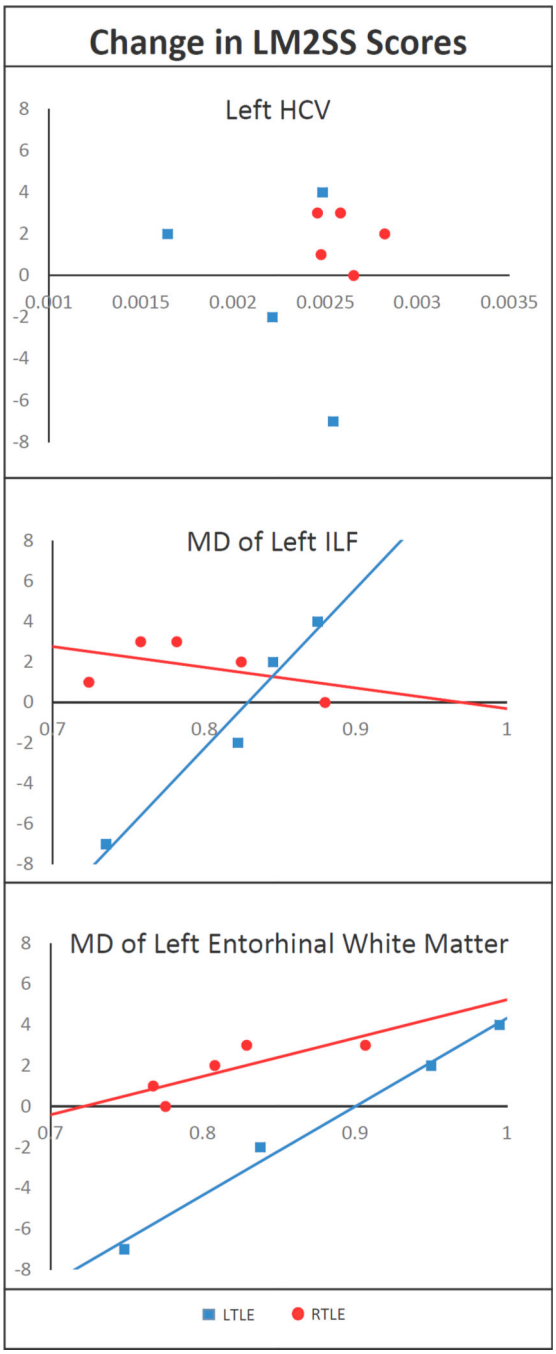

Figure 3.

Scatterplots depicting the relationship between pre- to post-surgical change in LM II scores and preoperative MD of the left HCV (top), MD of the left ILF (middle) and MD of the left entorhinal white matter (bottom) for patients with LTLE and RTLE. Postoperative data were not available for any of the patients with bilateral IAP or left-handedness.

Table 1

Demographic, seizure-related, and memory data for the patient and control sample

	LTLE (n=13)	RTLE (n=13)	Controls (n=35)
Age	36.59(13.29)	37.1(12.45)	38.2(12.17)
Years of education	13.54(1.61)	13.69(1.31)	14.91(2.09)
Gender (female/male)	9/4	7/6	22/13
Left hippocampal volume (mm3)	2757.92*†	3977.77	3892.28
Right hippocampal volume (mm3)	3868.64	3448.31*	3961.34
Age of seizure onset	15.38(13.88)	13.00(11.74)	-
Duration of illness (years)	21.23(11.29)	23.08(15.33)	-
Seizure frequency (/month)	8.46(9.25)	4.83(3.79)	-
Number of anticonvulsant meds	2.31(.86)	2.31(.63)	-
Number of patients with MTS	11	7	-
History of febrile seizure	1	2	-
LM 1 scaled score	6.92(2.63)*†	8.92(1.94)*	10.83(2.58)
LM II scaled score	6.08(3.10)*†	9.08(1.89)*	11.46(2.55)

The data represent means followed by standard deviations in parentheses.

* patient group mean differs from controls at $p < .05$

† LTLE group mean differs from RTLE group mean at $p < .05$

Table 2

Age-adjusted correlations between MRI variables and verbal memory scores

MRI Measures	Logical Memory I	Logical Memory II
Fiber Tract MD		
Left IFOF	−0.390	−0.615**
Right IFOF	−0.320	−0.602**
Left ILF	−0.510*	−0.699**
Right ILF	−0.378	−0.597*
Left FxC	0.148	−0.376
Right FxC	−0.234	−0.390
Left PHC	−0.229	−0.544*
Right PHC	−0.227	−0.444
Left UNC	−0.326	−0.587*
Right UNC	−0.276	−0.541*
Pericortical Diffusion		
Left MTL	−0.418	−0.606**
Right MTL	−0.179	−0.349
Left LTL	−0.373	−0.607**
Right LTL	−0.318	−0.497*
Cortical Diffusion		
Left MTL	−0.208	−0.380
Right MTL	−0.110	−0.322
Left LTL	−0.368	−0.596*
Right LTL	−0.316	−0.481
Cortical Thickness		
Left MTL	0.364	0.234
Right MTL	0.154	0.068
Left LTL	0.154	0.146
Right LTL	−0.044	−0.002
Cortical Contrast		
Left MTL	−0.054	0.079
Right MTL	0.139	0.117
Left LTL	0.127	0.056
Right LTL	0.084	0.095

MD = mean diffusivity; FxC= Fornix excluding fimbria, IFOF= Inferior Fronto-Occipital Fasiculus, ILF= Inferior Longitudinal Fasiculus, PHC= Parahippocampal Cingulum, UNC=Uncinate, MTL= medial temporal lobe, LTL= lateral temporal lobe.

* p<.0125,

** p<.005